Pathological but Not Physiological Retinal Neovascularization Is Altered in TNF-Rp55-Receptor–Deficient Mice

Norbert Kociok,[1,2,3] *Sven Radetzky,*[1] *Tim U. Krohne,*[1] *Claudia Gavranic,*[1,2] *and Antonia M. Joussen*[1,2,3]

Purpose. Tumor necrosis factor (TNF)-α is one of the major cytokines in inflammation and apoptosis. It has been demonstrated that inhibition of TNFα can reduce leukocyte adhesion, vascular leakage, and apoptotic endothelial cell death in diabetes. This study was conducted to investigate the effect of TNF-Rp55 and TNF-Rp75 on retinal development in oxygen-induced retinopathy.

Methods. TNF-Rp55– and TNF-Rp75–deficient mice, as well as their respective wild-type controls, were exposed to 75% oxygen from postnatal day P7 to P12. Retinal vascularization was investigated in flatmount preparations after concanavalin A labeling of endothelial cells on days P6, P14, P17, and P20. Retinal mRNA expression of VEGF, angiopoietin-1 and -2, and PDGF was examined at days P14 and P20.

Results. TNF-Rp55– and TNF-Rp75–deficient mice demonstrated similar retinal development and vascularization under normoxic conditions. In comparison to wild-type mice, the vascularized area remained stable during the observation time, although the gene expression of VEGF, angiopoietin (ang)-1 and -2, and PDGFb changed. Compared with that in the wild type mice, the relative expression of VEGF, ang-1, ang-2, and PDGFb changed 5.14-, 1.7-, 0.39-, and 0.36-fold in $Rp55^{-/-}$ mice and 4.1-, 9.5×10^{-5}-, 0.12-, and 2975-fold in $Rp75^{-/-}$ mice, respectively. Treatment with oxygen resulted in a significantly reduced vascularization in $Rp55^{-/-}$ but not $Rp75^{-/-}$ mice on postnatal day (P)20.

Conclusions. Inhibition of TNFα via TNF-Rp55 can alter retinal development and angiogenesis in a model of oxygen-induced retinopathy. The data underscore the potential effectiveness of TNF-inhibitory treatments as modulators in oxygen-induced retinopathy. (*Invest Ophthalmol Vis Sci.* 2006;47:5057–5065) DOI:10.1167/iovs.06-0407

Tumor necrosis factor (TNF)-α is one of the major cytokines in inflammation and apoptosis, with distinct anti- or proangiogenic effects.[1] Previous studies have shown that TNFα expression is increased in proliferative eye diseases in humans and retinal neovascularization in animal models.[2,3] TNF functions through a 55- and a 75-kDa receptor. Rp55 is involved in apoptosis and NFκB activation, and Rp75 is affiliated to lymphocyte proliferation.[4] In a murine mouse model of retinal neovascularization a significant increase of TNFα was found during the early hypoxic stimulus after oxygenation.[5] TNFα can reduce leukocyte adhesion and vascular leakage,[6] as well as apoptotic endothelial cell death in experimental diabetes. Inhibition of TNFα by semapimod, a translational inhibitor of TNFα,[7,8] in a mouse model of oxygen-induced retinopathy has been shown to improve physiological angiogenesis and to reduce pathologic neovascularization.[9]

The model of oxygen-induced retinopathy (OIR) in neonatal mice is widely used to analyze hypoxia-driven retinal neovascularization.[10–13] When the mice are returned to normoxia, the lack of retinal vessels in this model causes hypoxia, which strongly induces the release of angiogenic growth factors of the VEGF family such as VEGF-A and PDGF[14] and stimulates pathologic vasoproliferation at the junction of the avascular and vascularized retina.[11,15]

The periods of normal vascular pruning and pathologic vaso-obliteration are restricted to a temporal "plasticity window" that coincides with the formation of a pericyte-poor vasculature.[16] Platelet-derived growth factor β (PDGFb) promotes cellular proliferation and inhibits apoptosis. Lindahl et al.[17] found that mouse embryos deficient in PDGFb lack microvascular pericytes and develop numerous capillary microaneurysms that rupture in late gestation. Endothelial cells of the sprouting capillaries in mutant mice appear to be unable to attract PDGF-receptor-β–positive pericyte progenitor cells.

Besides PDGF, VEGF-induced angiogenesis has been shown to be facilitated by angiopoietin (ang)-1 and -2, both ligands of the Tie2 receptor.[18,19] Ang-1 promotes the maturation of the vascular network, and ang-2 initiates angiogenesis by destabilizing existing vessels.[20]

Although inflammation has recently been discussed in the context of hypoxia-induced neovascularization,[21] the interaction between inflammatory cytokines and the growth-factor panel involved in hypoxia is not yet understood. In the present study we investigated the effect of the lack of TNF-Rp55 or TNF-Rp75 on retinal development in mice in normal conditions and in oxygen-induced retinopathy, with respect to the retinal expression of VEGF, angiopoietins, and PDGF mRNA.

Methods

All animal experiments adhered to the ARVO Statement for the Use of Animals in Ophthalmic and Vision Research and were approved by the Animal Care and Use Committee of the Regierungspräsidium, Cologne, Germany.

C57BL/6 and knockout mice for Rp55 ($Rp55^{-/-}$) and Rp75 ($Rp75^{-/-}$) backcrossed to the C57/Bl6 background (Jackson Laboratory, Bar Harbor, ME) were used in the experiments. Animals were held in mating pairs and fed regular laboratory chow and water ad libitum. A 12-hour day–night cycle was maintained. For the oxygen

From the [1]Department of Vitreoretinal Surgery, Center for Ophthalmology, and the [2]Center for Molecular Medicine, University of Cologne, Cologne, Germany; and [3]Department of Ophthalmology, Heinrich-Heine University, Düsseldorf, Germany.

Supported by the Kämpgen Stiftung, Köln; Köln Fortune, University of Cologne, Deutsche Forschungsgemeinschaft (DFG) Grant Jo 324/6-2 (Emmy-Noether Program), and DFG Jo 324/10-1.

Submitted for publication April 11, 2006; revised June 16, 2006; accepted August 17, 2006.

Disclosure: **N. Kociok**, None; **S. Radetzky**, None; **T.U. Krohne**, None; **Gavranic**, None; **A.M. Joussen**, None

The publication costs of this article were defrayed in part by page charge payment. This article must therefore be marked "*advertisement*" in accordance with 18 U.S.C. §1734 solely to indicate this fact.

Corresponding author: Antonia M. Joussen, Department of Ophthalmology, Heinrich-Heine Univeristy, Moorenstr. 5, 40225 Düsseldorf, Germany; joussena@googlemail.com.

experiments, mice were kept in their cages in a chamber in which the oxygen partial pressure was maintained at 75%. The pressure was continuously checked and regulated by a digital oxymeter (GMH 3690 GL; Greisinger Electronic GmbH, Regenstauf, Germany).

Mouse Model of Oxygen-Induced Retinopathy

To induce reproducible proliferative retinal neovascularization in retinopathy of prematurity the protocol of Smith et al.[10] was performed under modified conditions. Mice—the nursing dam and her newborn pups—were housed in room air from postnatal day (P)0 to P7. On P7, pups of every group were exposed along with their nursing dams to 75% oxygen for 5 days and then transferred back to room air. Surrogate dams were provided if nursing dams died—a rare occurrence. Control mice were maintained in room-air up to P12. Pups were removed from their cages for analysis of retinal neovascularization on days P6, P14, P17, and P20. All experiments were performed in duplicate with a minimum number of five animals per group for each time point.

Visualization of Retinal Vascularization

Deep anesthesia was induced by intraperitoneal injection of ketamine (1%), xylazine (0.1%), and sodium chloride (0.9%) in a concentration of 0.1 mL/10 g mouse body weight. Sternotomy was performed to install a 22-gauge IV catheter (Venflon; BE Biosciences, Stockholm, Sweden) into the aorta via the left heart chamber. Perfusion started with a 1.5-mL sodium chloride 0.9% solution was followed by 1 mL paraformaldehyde 1%, and 1.5 mL of fluorescein concanavalin A 5% (Vector Laboratories, Burlingame, CA) and by a final perfusion with sodium chloride 0.9%. The eyes were enucleated and retinal flatmounts were prepared. The cornea was dissected with a circumferential limbal incision, followed by removal of the lens and vitreous. The open eyecup was inserted in a 1% PFA solution for 20 minutes. Four radial cuts helped to lift the retina from the underlying choroidea and sclera and to flatten it on a glass slide.

Quantification of Retinal Vascularization

Images of the perfused retinas were captured with a charge-coupled device (CCD) camera (C4742-95-12ER; Hamamatsu, Hamamatsu City, Japan) attached to a microscope (model MZ FLIII; Leica Microsystems, Bensheim, Germany). The images were captured on a computer (G4 Computer; Apple, Cupertino, CA) and analyzed (OpenLab software; Improvision Inc., Lexington, MA). The vascular area was quantified by setting a threshold level of fluorescence, above which only vessels were captured (density slicing). The entire mounted retinas were analyzed in a masked fashion to minimize sampling bias. The total surface area of the retina was outlined using the outermost vessel of the arcade near the ora serrata as the border. The total vascularized area was then normalized to the total retinal area and the percentage of the retina covered by vessels was calculated. Avascular areas were circumscribed manually and the percentage calculated as described.

All retinas were photographed with a standardized technique to compare vascular density and to analyze areas of neovascularization.

RNA Isolation and RT-PCR

Eye cups of anesthetized mice were removed as described. The whole retinas were homogenized (Lysisbuffer RNeasy Kit; Qiagen, Hilden Germany) and stored at −20°C until RNA isolation. RNA isolation and cDNA synthesis were performed according to the recommendations of the manufacturer (Qiagen).

The mRNA levels for VEGF, ang-1 and -2, PDGFb, and GAPDH in the mouse retinas after oxygenation were compared to retinas of mice kept in normal room oxygenation by real-time RT-PCR using a nucleic acid stain (SYBR Green I; Invitrogen-Molecular Probes, Eugene, OR) on a thermal cycler (iCycler; Bio-Rad Laboratories, Hercules, CA). Using primer analysis software (Oligo ver. 4.1; National Biosciences, Plymouth, MN), we selected gene specific primers suitable for real-time RT-PCR (*VEGF*: CAG CTA TTG CCG TCC GAT TGA GA and TGC TGG CTT TGG TGA GGT TTG AT; *ANG-1*: CTG ATG GAC TGG GAA GGG AAC C and CGC AGA AAT CAG CAC CGT GTA AG; *ANG-2*: GAA GGA CTG GGA AGG CAA CGA and CCA CCA GCC TCC TGA GAG CAT C; *PDGFb*: CAG GGA GCA GCG AGC CAA GA and CGG ACG AGG GGA ACA ACA TTA TCA; *GAPDH*: AAC TTT GTG AAG CTC ATT TCC TGG TAT and CCT TGC TGG GCT GGG TGG T). With these primers, the mRNA expression of VEGF, ang-1, -2, and PDGFb, together with GAPDH as the calibrator, were analyzed simultaneously in quadruple reactions according to the recommendations of the manufacturer (Qiagen). The analysis was repeated at least two times. Detection of the fluorescence product was performed during the last 90% of the cycles. To confirm amplification specificity, the PCR products from each primer pair were subjected to a melting-curve analysis (data not shown). Genomic DNA contamination was excluded by choosing primers hybridizing to different exons. Moreover, control amplification reactions were performed with nontranscribed RNA, as the templates gave only background fluorescence. The quantification data were analyzed with the thermal cycler system software (iCycler iQ; Bio-Rad Laboratories), as described.[22] The comparative C_T (threshold cycle, C_T) method was used for quantification of the target genes relative to GAPDH.

Using the geNorm calculation tool V3.3 (geNorm.xls), based on the method of Vandesompele et al.,[23] the expression of 12 calibration genes mentioned in this article was tested in our system. *GAPDH* belonged to the three most stable genes in our system and was used to normalize the expression levels of all genes.

Statistical Analysis

All results are expressed as the mean ± SD or mean normalized expression (MNE) ± SE for real-time RT-PCR results. After a normal distribution test (Shapiro-Wilks) the data were compared by unpaired *t*-test if the Levenne test showed equal variance. Otherwise, a nonparametric test (Mann-Whitney) was used. The data of the real-time RT-PCR (mean normalized expression ± 2× SE) were analyzed by Mann-Whitney test. Differences were considered statistically significant at $P < 0.05$.

Results

Vascular Development

Figures 1 to 4 illustrate the time course of retinal vascularization in wild-type, $Rp55^{-/-}$, and $Rp75^{-/-}$ mice, with or without oxygen treatment, in retinal flatmounts of concanavalin A-FITC–perfused animals. On P6, in all three groups the vascularization front starting at the center of the retina reached to only two thirds of the retina, leaving the outer retina completely avascular (Fig. 1). Formation of the capillary network began after the main vessels had reached half of the distance to the outer frontier of the retina. At this point, avascular areas around the optic nerve persisted.

Without oxygen treatment, the formation of the retinal capillaries was complete on P14 in all three groups (Figs. 2A–C). At this time point, the main vessels as well as the fine capillaries had reached the outer edge of the retina, and the area around the optic nerve was fully vascularized. There was no further capillary growth from day P17 onward in all three groups (Figs 3, 4A–C).

In contrast, after oxygen treatment, the vascularization on P14 was retarded in all three groups. On P6, the main vessels with their capillaries had reached the outer edge of the retina; however, great parts of the central retina around the optic nerve remained nonvascularized compared with age-matched control subjects held in normoxia (Figs. 2D–F). Pathologic neovascular tufts were apparent at the outer edge of the retina at this stage. On P17, the avascular area around the optic nerve decreased because of the growing capillary network in all

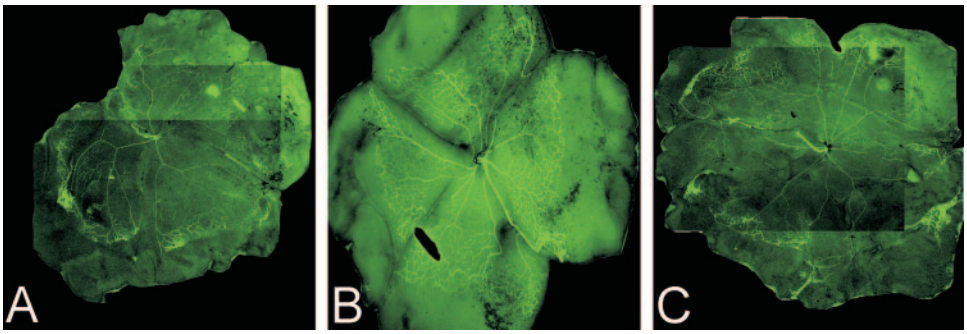

FIGURE 1. Retinal flatmounts at P6 from wt C57BL/6 (**A**), Rp55$^{-/-}$ (**B**), and Rp75$^{-/-}$ (**C**) mice.

three groups, although there were still many neovascular tufts (Figs. 3D–F).

On P20, Rp55$^{-/-}$ mice clearly differed from both wild-type and Rp75$^{-/-}$ mice. Whereas the avascular area around the optic nerve had been closed by capillaries in the wild-type and the Rp75$^{-/-}$ mice, these avascular areas persisted in Rp55$^{-/-}$ mice (Figs. 4D and 4F versus 4E). In addition, the neovascular tufts at the outer edge of the retina remained prominent in Rp55$^{-/-}$ mice In Rp75$^{-/-}$ mice, the neovascular tufts are reduced in number and size on P20 and nearly gone in wild-type mice.

The development of retinal vasculature was quantified by comparing the vascularized areas as a percentage of the total retinal surface. After a tremendous increase in vessel formation until P14, vascularization of wild-type retinas was almost completed (41.7% ± 9.4%; vascularized area in relation to the total retinal area) and remained stable until P20. Without oxygen treatment, both Rp55 and Rp75 knockout mice showed a similar vascularization pattern as demonstrated in Fig. 5. Only in the Rp75$^{-/-}$ group did vascularization increase (to 54.3% ± 2.2% on P17), but it deteriorated again to 46.9% ± 2% at P20.

In contrast, a retardation of retinal vascularization was observed after oxygen treatment. Whereas the vascularized area was 16.3% ± 3.1% on P14 in wild-type mice and remained stable until P17, vascularization increased to 37.2% ± 1.8% on P20.

Starting on P14 an until P20, vascularization was significantly lower in Rp55$^{-/-}$ mice than in their wild-type controls (P14, 8.7% ± 3%; P20, 18.4% ± 6.2%, respectively; $P < 0.01$). In contrast, there was a major increase in vascularization within the Rp75$^{-/-}$ group from P14 to P20 reaching the wild-type level of vascularization (P14, 9.4% ± 6%, P20, 46.2% ± 4.5%, respectively). On P20, vascularization of wild-type mice and Rp75$^{-/-}$ mice reached the level of non-oxygen–treated animals (~40%), whereas the vascularization of the Rp55$^{-/-}$ mice did not improve from P17 to P20 and remained constant at approximately 20%.

When analyzing the avascular area in relation to the total retinal area, it was striking that the avascular area in animals without oxygen treatment was already very low at P14 in all three groups and persisted at this level until P20 (Fig. 6).

As expected, with oxygen treatment, the percentage of the avascular area was initially higher and decreased from 25.6% ± 6% and 34% ± 4.4% at P14 to 16.2% ± 8.8% and 11.8% ± 3.6% on P17 in wild-type animals and Rp75$^{-/-}$ mice, respectively. There was virtually no avascular zone present at P20. In Rp55$^{-/-}$ mice the avascular zone starting with 32.2% ± 1% at P14 persisted at 20.2% ± 2.1% on P17 and 13.7% ± 7.8% on P20.

mRNA Expression of VEGF, Ang-1, Ang-2, and PDGFb during Retinal Vascular Development under Normoxic Conditions

To evaluate the mRNA expression of VEGF, ang-1, ang-2, and PDGFb in the retina, we performed real-time PCR. The GAPDH-

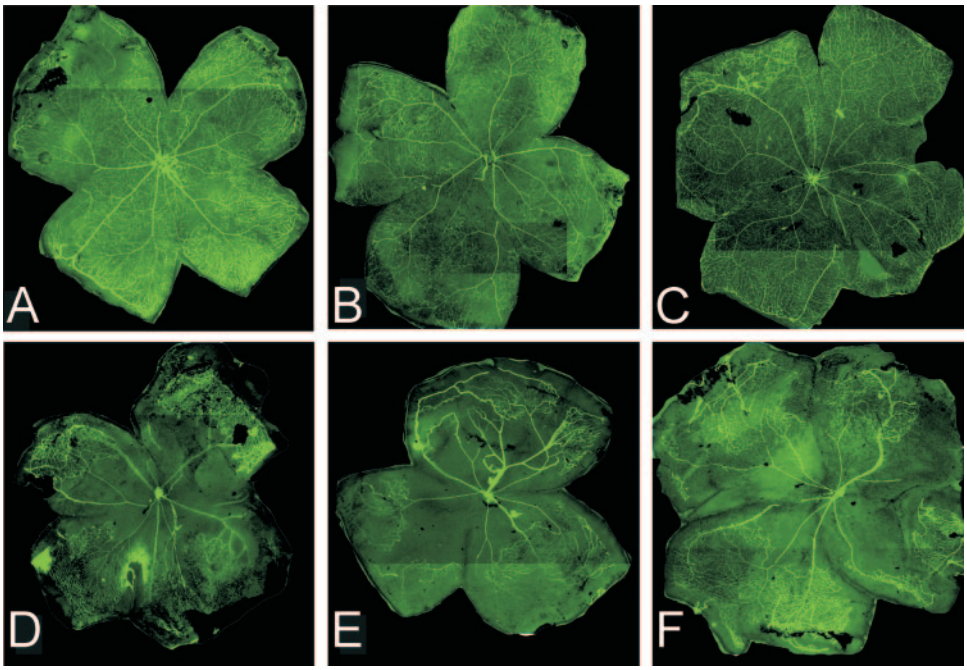

FIGURE 2. Retinal flatmounts at P14 from wt C57BL/6 (**A**, **D**), Rp55$^{-/-}$ (**B**, **E**), and Rp75$^{-/-}$ (**C**, **F**) mice after normoxia (**A–C**) and after oxygen treatment (**D–F**).

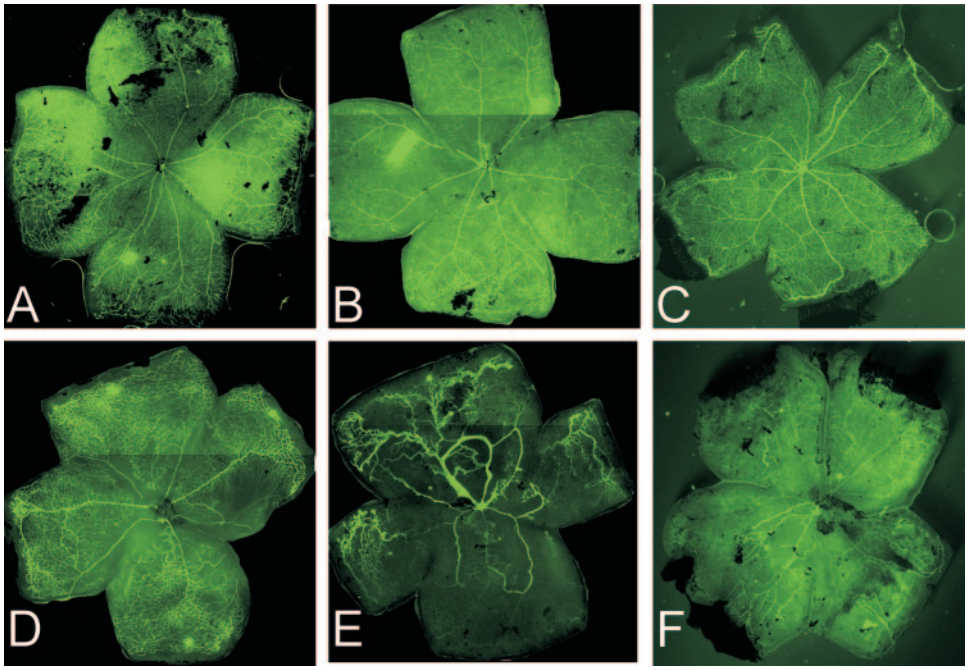

FIGURE 3. Retinal flatmounts at P17 from wt C57BL/6 (**A**, **D**), Rp55$^{-/-}$ (**B**, **E**), and Rp75$^{-/-}$ (**C**, **F**) mice after normoxia (**A–C**) and after oxygen treatment (**D–F**).

calibrated normoxic mRNA expression levels and the relative expression, normalized to the expression in the wild type on P14, are shown in Table 1.

Even under normoxic conditions, there were large differences in the VEGF mRNA level between the genotypes. The highest mean normalized mRNA expression in the wild type at baseline (P14) was measured for VEGF. Compared with wild-type mice, VEGF mRNA expression on P14 was approximately five times higher in Rp55$^{-/-}$ mice and approximately four times higher in Rp75$^{-/-}$ mice.

During normal retinal development, VEGF mRNA in wild-type animals increased approximately sevenfold between P14 and P20. This increase was modulated in both TNFα receptor knockout mice. In mice lacking Rp75, the initially higher VEGF mRNA level remained mostly constant, but in mice lacking Rp55, the VEGF mRNA level decreased below the initial value of wild-type mice (Fig. 7A).

The ang-1 mean normalized mRNA expression in the wild type was determined with 1.5E−05 ± 1.5E−06. The ang-1 mRNA expression was only slightly increased in Rp55$^{-/-}$ mice but was dramatically decreased to nearly 0 in Rp75$^{-/-}$ mice (Table 1). There were large qualitative and quantitative differences in the mRNA level of ang-1 in both TNFα receptor deficient mice. In C57 mice the amount increased only about a factor 4, from P14 to P20. If Rp55 was missing, the increase started from a 1.7 times higher value at P14 and increased further by a factor of ~11 toward P20. Likewise, in Rp75$^{-/-}$ mice there was a large increase in the ang-1 mRNA level from

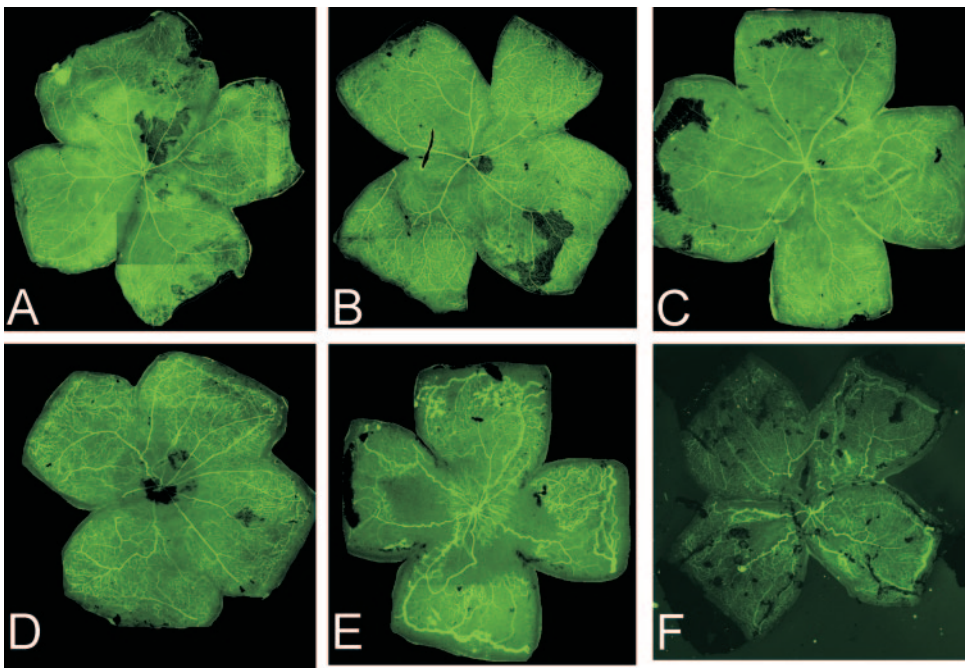

FIGURE 4. Retinal flatmounts at P20 from wt (**A**, **D**), Rp55$^{-/-}$ (**B**, **E**), and Rp75$^{-/-}$ (**C**, **F**) mice after normoxia (**A–C**) and after oxygen treatment (**D–F**).

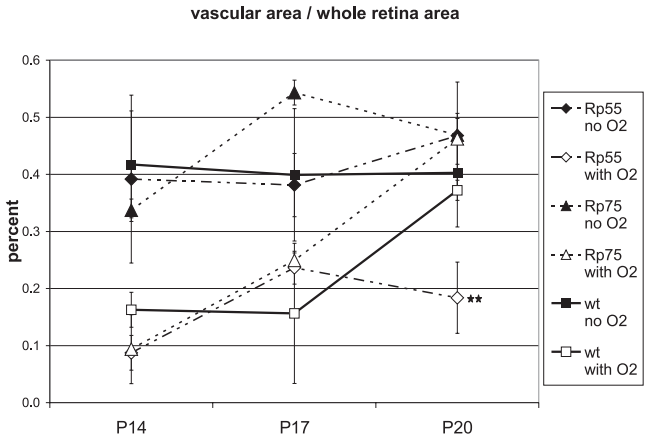

FIGURE 5. Vascular area as a percentage of the whole retina at P14, P17, and P20 in wt, $Rp55^{-/-}$, and $Rp55^{-/-}$ mice, after normoxia conditions and after oxygen treatment. There is a significant difference between the mean vascular area of C57 wild type and $Rp55^{-/-}$ mice ($P < 0.01$).

P14 to P20, but the increase started at a 10,000-fold lower level at P14 compared with the C57 wild type. (Fig. 7C).

In wild-type animals the mean normalized expression of ang-2 was very low: 3E−10 ± 5.9E−11 (Table 1), and even lower in $Rp55^{-/-}$ mice and $Rp75^{-/-}$ mice (Fig. 7E). Both knockout mice showed a constant ang-2 mRNA expression at this low level at P20 compared with P14, whereas in C57 wild-type mice the ang-2 expression increased 12-fold.

Similarly, the mean normalized expression of PDGFb was very low: 2.3E−10 ± 7.3E−11 (Table 1) and even decreased to a third in $Rp55^{-/-}$ mice. In contrast, PDGFb expression in $Rp75^{-/-}$ mice increased nearly 3000-fold compared with the C57 wild-type control animals at P14. In all three analyzed genotypes, the PDGFb expression increased from P14 to P20 (Fig. 7G).

When summarizing the mRNA expression during normoxia, both knockout mice exerted a qualitatively, but not quantitatively, similar pattern concerning the expression of ang-1, ang-2, and PDGFb that differed from the expression in C57 wild-type animals. This result was in contrast to the VEGF mRNA expression pattern. VEGF mRNA expression in $Rp75^{-/-}$ mice was similar to that in the wild-type animals, whereas in $Rp55^{-/-}$ mice VEGF it was oppositely regulated during development (Fig. 7A–G).

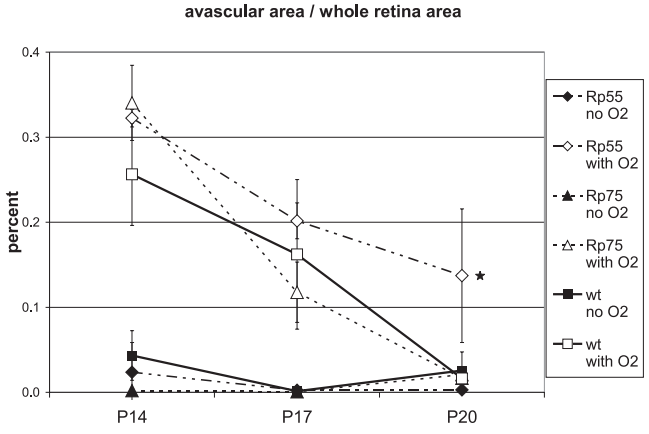

FIGURE 6. Avascular area as a percentage of the whole retina at P14, P17, and P20 in wt, $Rp55^{-/-}$, and $Rp75^{-/-}$ mice after normoxia and after oxygen treatment. There is a significant difference between the mean avascular area of C57 wild type and $Rp55^{-/-}$ mice: $P < 0.05$.

TABLE 1. Mean Normalized mRNA Expression on P14 for VEGF, ANG1, ANG2, and PDGFb in Normoxic Conditions

	VEGF			Ang-1			Ang-2			PDGFb		
	MNE	SEM of MNE	MNE Calibrated to C57	MNE	SEM of MNE	MNE Calibrated to C57	MNE	SEM of MNE	MNE Calibrated to C57	MNE	SEM of MNE	MNE Calibrated to C57
C57	5.36E−04	4.39E−05	1.00	1.50E−05	1.51E−08	1.00	3.09E−10	5.86E−11	1.00	2.27E−10	7.29E−11	1.00
$Rp55^{-/-}$	2.75E−03	3.32E−04	5.14	2.55E−05	2.67E−08	1.70	1.20E−10	3.13E−11	0.39	6.24E−11	1.64E−11	0.36
$Rp75^{-/-}$	2.20E−03	4.72E−04	4.10	1.42E−09	3.64E−10	0.000095	3.57E−11	1.08E−11	0.12	6.76E−07	1.99E−07	2975

	VEGF			Ang-1			Ang-2			PDGFb		
	MNE	SEM of MNE	MNE Calibrated to C57	MNE	SEM of MNE	MNE Calibrated to C57	MNE	SEM of MNE	MNE Calibrated to C57	MNE	SEM of MNE	MNE Calibrated to C57
C57	5.36E−04	4.39E−05	1.00	1.50E−05	1.51E−08	1.00	3.09E−10	5.86E−11	1.00	2.27E−10	7.29E−11	1.00
$Rp55^{-/-}$	2.75E−03	3.32E−04	5.14	2.55E−05	2.67E−08	1.70	1.20E−10	3.13E−11	0.39	6.24E−11	1.64E−11	0.36
$Rp75^{-/-}$	2.20E−03	4.72E−04	4.10	1.42E−09	3.64E−10	0.000095	3.57E−11	1.08E−11	0.12	6.76E−07	1.99E−07	2975
			SEM of MNE Calibrated to C57			SEM of MNE Calibrated to C57			SEM of MNE Calibrated to C57			SEM of MNE Calibrated to C57
C57			0.12			0.14			0.27			0.45
$Rp55^{-/-}$			0.75			0.25			0.12			0.14
$Rp75^{-/-}$			0.94			0.000026			0.04			1294

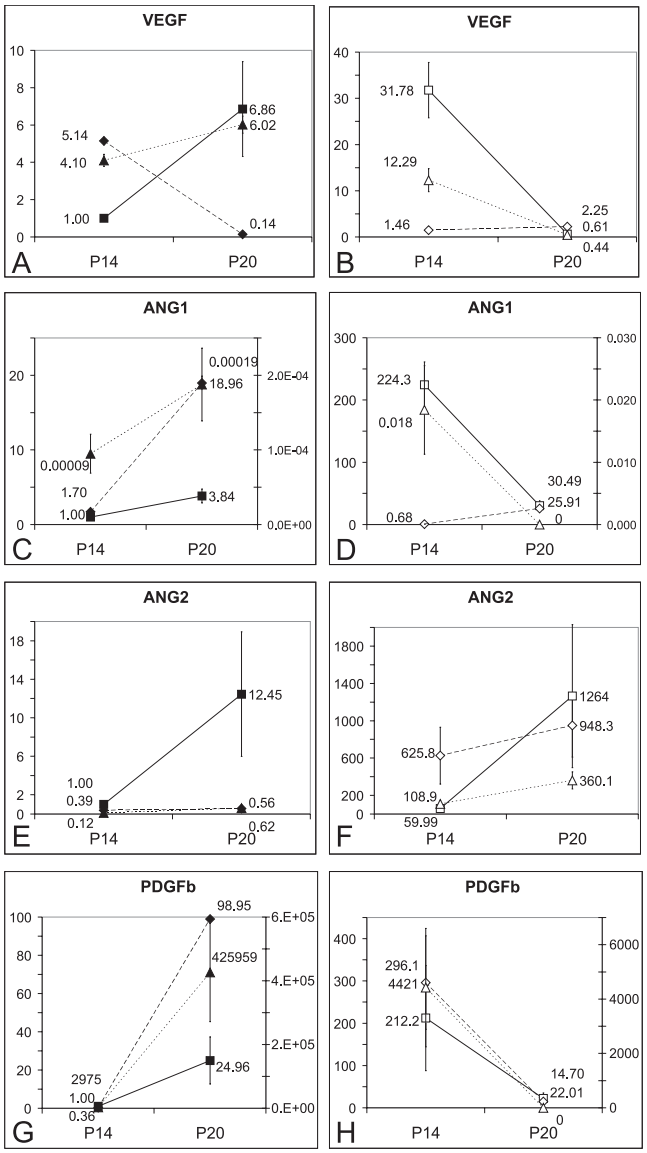

FIGURE 7. Mean normalized expression of VEGF, ang-1, ang-2, and PDGFb mRNA at P14 and P20 after normoxic conditions (**A**, **C**, **E**, **G**) and after oxygen treatment (**B**, **D**, **F**, **H**). The expression is calibrated to the wt MNE of each gene at P14 (set a 1). *Squares*: wt; *diamonds*: Rp55$^{-/-}$; *triangles*: Rp75$^{-/-}$ Because the relative expression of ang-1 and PDGFb in retinas of Rp75$^{-/-}$ was very different from the expression of wt and Rp55$^{-/-}$, a secondary *y*-axis was used (*right*).

Influence of Hypoxia on the mRNA Levels of VEGF, Ang-1, Ang-2, and PDGFb

As expected, oxygen treatment followed by relative hypoxia resulted in a large increase (32-fold) of the VEGF mRNA in wild-type mice on P14, deteriorating to baseline at P20 (Fig. 7B). Of note, hypoxia had no influence on the VEGF mRNA expression in Rp55$^{-/-}$ mice: It remained nearly constant from P14 to P20 at a threefold lower level compared with normoxic conditions at P14 (Fig. 7B). In Rp75$^{-/-}$ mice VEGF mRNA expression increased only slightly (threefold) after oxygen treatment on P14 compared with the normoxic conditions and declined to 10% of the normoxic level on P20 (Fig. 7B). The mRNA expression level in Rp75$^{-/-}$ mice after oxygen treatment was comparable to the baseline expression in wild-type animals.

Relative hypoxia increased the ang-1 mRNA expression in the C57 wild type approximately 225-fold, compared with the expression of the normoxic level at P14, and deteriorated to a 30-fold level at P20 (Fig. 7D). In Rp55$^{-/-}$ mice, in contrast with the expression in wild-type animals, there was no increased ang-1 mRNA level at P14 but even a decreased level compared with the situation in normoxia (Figs. 7C, 7D). From P14 to P20 there was a 40-fold increase in the ang-1 mRNA expression in Rp55$^{-/-}$ mice, resulting in a similar level at P20 compared with the wild type. The ang-1 mRNA expression in Rp75$^{-/-}$ mice resembled the situation in the wild type not in a quantitative but in a qualitative way. At P14 the ang-1 mRNA level was 200-fold higher in the hypoxic situation than under normoxic conditions, as it was in the wild type. As in the wild type, the mRNA level then decreased at P20 in Rp75 mice to a virtually unmeasurable level (Fig. 7B).

The ang-2 mRNA expression in wild-type mice at P14 was elevated 60-fold in relative hypoxia compared with the normoxic situation and further increased by 20-fold at P20. Rp55$^{-/-}$ mice in hypoxia were measured to have 1600 times the P14-normoxic ang-2 mRNA expression, and the level increased 1.5-fold at P20. Similarly, the Rp75$^{-/-}$ mice started with a 1000-fold elevated level of ang-2 mRNA at P14 compared with the level at normoxia and increased this level further (factor of ~3 at P20; Fig. 7F).

Under hypoxia, all three analyzed genotypes started with elevated PDGFb mRNA levels at P14 compared with the normoxic situation. Whereas for the wild type this elevated level in hypoxia was 200-fold higher than in normoxia, it was 800-fold higher for the Rp55$^{-/-}$ mice and only 1.5-fold higher for the Rp75$^{-/-}$ mice (Fig. 7H), although in Rp75$^{-/-}$ mice the normoxic level at P14 was 3000-times higher than in the wild type (Fig. 7G), resulting in a 20-fold higher PDGFb mRNA level for the Rp75$^{-/-}$ mice at hypoxia at P14 compared with the wild-type and the Rp55$^{-/-}$ mice. In all three genotypes, the PDGFb mRNA level decreased sharply under hypoxia at P20. In the C57 wild type this decrease was 10-fold, in the Rp55 mice 20-fold, and in the Rp75 mice the decrease was more than 4400-fold, resulting in an immeasurable expression at P20.

DISCUSSION

In the present study, TNF-Rp55– and TNF-Rp75–deficient mice exerted a similar retinal development and vascularization under normoxic conditions, although the gene expression of VEGF, ang-1, ang-2, and PDGFb varied considerably as measured at P14 and P20. Under hypoxic conditions all groups demonstrated a significant enlargement of retinal vessels with formation of neovascularization early after oxygen treatment. Treatment with oxygen resulted in a reduced vascularization in TNF-Rp55– but not TNF-Rp75–deficient mice on P17 and P20, indicating that inhibition of TNFα via TNF-Rp55 can alter retinal development and angiogenesis in a model of oxygen-induced retinopathy.

These data are in accordance with the data published recently by Ilg et al.,[24] demonstrating that in normoxia, B6129- and TNFR-deficient mice, lacking both TNF receptors, reveal a similar degree of normal retinal vascular development at the superficial vascular network, but a retarded development of the deep retinal vessels.

The formation of the vascular system is a complex process in which an initial plexus of endothelial cell tubes later becomes remodeled into a mature network.[25] Of interest, in normoxic conditions, we found an altered mRNA expression of VEGF, ang-1, ang-2, and PDGFb in the retina; however, no prominent alterations in vascularization were noted between wild-type and TNF-receptor–deficient mice. A possible expla-

nation is that the lower retinal plexus is still incomplete by P8, but is complete by P10.[16] Thus, at our observation point on P14, the initial retinal network was complete and not susceptible to cytokine alterations, although the pericyte coverage was still incomplete, and by P18 pericytes had reached secondary and tertiary branches, but did not fully cover the deep plexus at that stage.[16] In our experiments, vessels were labeled using perfusion with lectin, whereas staining with CD31 may have demonstrated proliferating and budding vascular endothelial cells that had not yet matured into a potent vessel. Nevertheless, this difference would be expected for all groups in the same manner.

VEGF expression increased during normal development from day 14 to 17 in our model and was, as expected, unidirectionally regulated with the expression of ang-1 and PDGF, both related to pericyte recruitment and assembly.

So far, it is assumed that TNF-influenced growth factor expression exerts its major effects on inflammatory interactions involving endothelial cells. In an unexpected finding in our model, neither of the TNF-receptor–deficient mice demonstrated a change in retinal vascular development under normoxic conditions. This is similar to the findings by Ilg et al.[24] in FITC-perfused retinas, qualitatively demonstrating similar degrees of vascular development and vaso-obliteration on P12 in room-air– and hyperoxia-exposed TNF-receptor–deficient and B6129 mice.[24] In hypoxia, the role of TNFα changed and $Rp55^{-/-}$ mice underwent a delayed vascularization, with both an altered development of the intraretinal vessels and the altered angiogenic response previously shown.[24] In our study this effect was seen only in $Rp55^{-/-}$ mice, but not in $Rp75^{-/-}$ mice.

TNFα has been shown to be proangiogenic in vivo,[26,27] through stimulation of VEGF induction.[28] We showed that TNFα stimulated VEGF expression via the Rp55-dependent pathway, as the VEGF mRNA level in $Rp75^{-/-}$ mice was similar to the wild-type level at P14 and P20, during normal vascular development in the retina. In contrast, the VEGF mRNA level decreased markedly in $Rp55^{-/-}$ mice, to one fiftieth of that in the wild-type mice at P20.

Little is known about the influence of TNFα on PDGFb expression. TNFα does not significantly affect PDGF α-receptor mRNA or protein expression, nor does it alter the proliferative response to externally added PDGF-AA in fibroblast cultures. In contrast, TNFα reduces the levels of PDGF β-receptor mRNA, protein expression, and cell proliferation in response to PDGF-BB. At the same time, TNFα may alter the response to PDGF-BB from exogenous sources.[29] We showed that during normal retinal development the presence of both TNF-receptors was necessary for a proper regulation of the PDGFb mRNA expression In C57 mice, the PDGFb mRNA expression increased moderately from P14 to P20. This increase was more than 10 times higher (275-fold) when the Rp55 receptor was missing, and the effect was even greater in $Rp75^{-/-}$ mice.

There is evidence that lipid hydroperoxide stimulates retinal neovascularization in rabbit retina through expression of TNFα, VEGF, and PDGF.[3] This is in accordance with our data, as we have shown that, under relative hypoxic conditions, the PDGFb mRNA level was dramatically reduced.

Ang-1 is thought not to be mitogenic in endothelial cells, but it stimulates endothelial cell migration and sprouting and, in this respect, is synergistic with VEGF.[30,31] Ang-1 in cooperation with VEGF plays a key role in vascular maturation and survival in vivo.[20,32–34] Whereas VEGF increases vascular permeability, ang-1 protects against VEGF-induced vascular leakage and strengthens junctions between endothelial cells.[35,36] Angiopoietins further promote acute recruitment of leukocytes, which may contribute to vascular remodeling and angiogenesis, and thus angiopioetins may be considered proinflammatory mediators.[37,38]

Only a little information is available about the factors that upregulate ang-1 expression. Ang-1 mRNA expression is sustained in response to VEGF and hypoxia in retinal microvascular endothelial cells.[39] The ang-1 receptor Tie2 is upregulated by hypoxia and inflammatory cytokines including TNFα.[40,41] Recently, it was shown that TNF-α upregulates ang-1 in cultured human synoviocytes[42] and in endothelial cells.[43] This finding is in accordance with our data in mice at P20. We showed that Rp75 is necessary for ang-1 expression, as nearly no ang-1 mRNA was detected in $Rp75^{-/-}$ mice, whereas the Rp55-receptor was not necessary for ang-1 transcription but for a proper regulation of ang-1 mRNA during normal angiogenesis in the retina as well as under hypoxic conditions.

In a rat model of ROP Sarlos et al.[44] have shown that ang-2 but not ang-1 is upregulated at P18. Ang-2 is thought to be angiogenic in vivo, as ang-2 enhances VEGF-mediated angiogenesis, probably by blocking the stabilizing or maturing function of ang-1, thus allowing vessels to respond better to a sprouting signal by VEGF.[18,20,45] Previous studies have shown that ang-2 mRNA is induced by basic fibroblast growth factor, VEGF, angiotensin II and hypoxia in bovine microvascular endothelial cells.[39,46–48]

The hypoxia-driven ang-2 expression may be independent of the HIF pathway and may depend on COX-2-dependent prostanoids.[49] Recently, it was shown that TNF-α upregulates ang-2 in human umbilical vein endothelial cells[50] and that the increase in ang-1 and ang-2 in bovine choroidal microvascular endothelial cells stimulated by TNF-α is due to an increase in ang-1 and ang-2 gene transcription.[43] However, from results in studies of ang-2–deficient mice, it has been concluded that ang-2 plays a critical role in physiologic and pathologic angiogenesis and in physiologic, but not oxygen-induced vascular regression in the eye.[51]

In our study ang-2 was markedly upregulated in the retina of C57 mice in normoxic conditions from P14 to P20. This regulation involved, at least partly, both TNF-receptors. Nevertheless, mice lacking Rp55 or Rp75 were able to react on relative hypoxic conditions from P14 to P20 as C57 mice did, although in a much reduced manner, indicating that additional pathways were involved in ang-2 expression regulation. Our data on the upregulation of ang-2 in C57 mice are confirmed by Sarlos et al.[44] They have shown that ang-2 and Tie2, but not ang-1 is upregulated in a rat ROP model. In addition, the inhibitory effect of hypoxia on the activity of the angiopoietin-1/Tie-2 receptor pathway through reduction of angiopoietin-1 and upregulation of angiopoietin-2 and -3 was shown in various organs of the rat.[52]

In our present study, we sought to identify the role of TNFα in the growth-factor and cytokine network involved in hypoxic neovascularization, but did not identify in detail the transcriptional pathways involved. Romashkova and Makarov[53] showed that PDGF activates the RAS/PIK3/AKT1/IKK/NFKB1 pathway. Similar regulatory mechanisms may be involved in hypoxic neovascularization and deserve further evaluation in the future. At this stage, our data support the importance of TNFα in retinal neovascularization and highlight the fact that different tightly regulated mechanisms are interweaved. Although it has been shown that inhibition and deletion of TNFα facilitates physiological angiogenesis within the ischemic retina, with a concomitant reduction in pathologic neovascularization of the vitreous body,[9] and TNFα inhibitors are tempting for the treatment of neovascular disease, further evaluation of the complicated molecular mechanisms is necessary.

References

1. Fajardo LF, Kwan HH, Kowalski J, Prionas SD. Dual role of tumor necrosis factor-alpha in angiogenesis. *Am J Pathol*. 1992;140:539–544.
2. Spranger J, Meyer-Schwickerath R, Klein M, Schatz H. [TNF-alpha level in the vitreous body. Increase in neovascular eye diseases and proliferative diabetic retinopathy]. *Med Klin* (*Munich*). 1995;90:134–137.
3. Armstrong D, Ueda T, Ueda T, Aljada A. Lipid hydroperoxide stimulates retinal neovascularization in rabbit retina through expression of tumor necrosis factor-alpha, vascular endothelial growth factor and platelet-derived growth factor. *Angiogenesis*. 1998;2:93–104.
4. Wallach D, Varfolomeev EE, Malinin NL, Goltsev YV. Tumor necrosis factor receptor and Fas signaling mechanisms. *Annu Rev Immunol*. 1999;17:331–367.
5. Majka S, McGuire PG, Das A. Regulation of matrix metalloproteinase expression by tumor necrosis factor in a murine model of retinal neovascularization. *Invest Ophthalmol Vis Sci*. 2002;43:260–266.
6. Joussen AM, Poulaki V, Mitsiades N, Kirchhof B. Nonsteroidal anti-inflammatory drugs prevent early diabetic retinopathy via TNF-alpha suppression. *FASEB J*. 2002;16:438–440.
7. Cohen PS, Nakshatri H, Dennis J, Caragine T. CNI-1493 inhibits monocyte/macrophage tumor necrosis factor by suppression of translation efficiency. *Proc Natl Acad Sci USA*. 1996;93:3967–3971.
8. Bianchi M, Bloom O, Raabe T, Cohen PS. Suppression of proinflammatory cytokines in monocytes by a tetravalent guanylhydrazone. *J Exp Med*. 1996;183:927–936.
9. Gardiner TA, Gibson DS, de Gooyer TE, de La Cruz V, McDonald DM, Stitt, AW. Inhibition of tumor necrosis factor-alpha improves physiological angiogenesis and reduces pathological neovascularization in ischemic retinopathy. *Am J Pathol*. 2005;166:637–644.
10. Smith LE, Wesolowski E, McLellan A, Kostyk SK. Oxygen-induced retinopathy in the mouse. *Invest Ophthalmol Vis Sci*. 1994;35:101–111.
11. Alon T, Hemo I, Itin A, Pe'er J. Vascular endothelial growth factor acts as a survival factor for newly formed retinal vessels and has implications for retinopathy of prematurity. *Nat Med*. 1995;1:1024–1028.
12. Stone J, Itin A, Alon T, Pe'er J. Development of retinal vasculature is mediated by hypoxia-induced vascular endothelial growth factor (VEGF) expression by neuroglia. *J Neurosci*. 1995;15:4738–4747.
13. Brooks SE, Gu X, Samuel S, Marcus DM. Reduced severity of oxygen-induced retinopathy in eNOS-deficient mice. *Invest Ophthalmol Vis Sci*. 2001;42:222–228.
14. Simpson DA, Murphy GM, Bhaduri T, Gardiner TA. Expression of the VEGF gene family during retinal vaso-obliteration and hypoxia. *Biochem Biophys Res Commun*. 1999;262:333–340.
15. Pierce EA, Avery RL, Foley ED, Aiello LP. Vascular endothelial growth factor/vascular permeability factor expression in a mouse model of retinal neovascularization. *Proc Natl Acad Sci USA*. 1995;92:905–909.
16. Benjamin LE, Hemo I, Keshet E. A plasticity window for blood vessel remodelling is defined by pericyte coverage of the preformed endothelial network and is regulated by PDGF-B and VEGF. *Development*. 1998;125:1591–1598.
17. Lindahl P, Johansson BR, Leveen P, Betsholtz C. Pericyte loss and microaneurysm formation in PDGF-B-deficient mice. *Science*. 1997;277:242–245.
18. Maisonpierre PC, Suri C, Jones PF, Bartunkova S. Angiopoietin-2, a natural antagonist for Tie2 that disrupts in vivo angiogenesis. *Science*. 1997;277:55–60.
19. Davis S, Aldrich TH, Jones PF, Acheson A. Isolation of angiopoietin-1, a ligand for the TIE2 receptor, by secretion-trap expression cloning. *Cell*. 1996;87:1161–1169.
20. Asahara T, Chen D, Takahashi T, Fujikawa K. Tie2 receptor ligands, angiopoietin-1 and angiopoietin-2, modulate VEGF-induced postnatal neovascularization. *Circ Res*. 1998;83:233–240.
21. Ishida S, Yamashiro K, Usui T, Kaji Y. Leukocytes mediate retinal vascular remodeling during development and vaso-obliteration in disease. *Nat Med*. 2003;9:781–788.
22. Morrison TB, Weis JJ, Wittwer CT. Quantification of low-copy transcripts by continuous SYBR Green I monitoring during amplification. *BioTechniques*. 1998;24:954–958,960,962.
23. Vandesompele J, De Preter K, Pattyn F, Poppe B. Accurate normalization of real-time quantitative RT-PCR data by geometric averaging of multiple internal control genes. *Genome Biol*. 2002;3:RESEARCH0034.
24. Ilg RC, Davies MH, Powers MR. Altered retinal neovascularization in TNF receptor-deficient mice. *Curr Eye Res*. 2005;30:1003–1013.
25. Risau W. Mechanisms of angiogenesis. *Nature*. 1997;386:671–674.
26. Frater-Schroder M, Risau W, Hallmann R, Gautschi P. Tumor necrosis factor type alpha, a potent inhibitor of endothelial cell growth in vitro, is angiogenic in vivo. *Proc Natl Acad Sci USA*. 1987;84:5277–5281.
27. Leibovich SJ, Polverini PJ, Shepard HM, Wiseman DM. Macrophage-induced angiogenesis is mediated by tumour necrosis factor-alpha. *Nature*. 1987;329:630–632.
28. Ryuto M, Ono M, Izumi H, Yoshida S. Induction of vascular endothelial growth factor by tumor necrosis factor alpha in human glioma cells: possible roles of SP-1. *J Biol Chem*. 1996;271:28220–28228.
29. Battegay EJ, Raines EW, Colbert T, Ross R. TNF-alpha stimulation of fibroblast proliferation. Dependence on platelet-derived growth factor (PDGF) secretion and alteration of PDGF receptor expression. *J Immunol*. 1995;154:6040–6047.
30. Koblizek TI, Weiss C, Yancopoulos GD, Deutsch U. Angiopoietin-1 induces sprouting angiogenesis in vitro. *Curr Biol*. 1998;8:529–532.
31. Witzenbichler B, Maisonpierre PC, Jones P, Yancopoulos GD. Chemotactic properties of angiopoietin-1 and -2, ligands for the endothelial-specific receptor tyrosine kinase Tie2. *J Biol Chem*. 1998;273:18514–18521.
32. Papapetropoulos A, Garcia-Cardena G, Dengler TJ, Maisonpierre PC. Direct actions of angiopoietin-1 on human endothelium: evidence for network stabilization, cell survival, and interaction with other angiogenic growth factors. *Lab Invest*. 1999;79:213–223.
33. Suri C, Jones PF, Patan S, Bartunkova S. Requisite role of angiopoietin-1, a ligand for the TIE2 receptor, during embryonic angiogenesis. *Cell*. 1996;87:1171–1180.
34. Vikkula M, Boon LM, Carraway KL, III, Calvert JT. Vascular dysmorphogenesis caused by an activating mutation in the receptor tyrosine kinase TIE2. *Cell*. 1996;87:1181–1190.
35. Gamble JR, Drew J, Trezise L, Underwood A. Angiopoietin-1 Is an antipermeability and anti-inflammatory agent in vitro and targets cell junctions. *Circ Res*. 2000;87:603–607.
36. Thurston G, Rudge JS, Ioffe E, Zhou H. Angiopoietin-1 protects the adult vasculature against plasma leakage. *Nat Med*. 2000;6:460–463.
37. Joussen AM, Poulaki V, Tsujikawa A, Qin W. Suppression of diabetic retinopathy with angiopoietin-1. *Am J Pathol*. 2002;160:1683–1693.
38. Lemieux C, Maliba R, Favier J, Theoret JF. Angiopoietins can directly activate endothelial cells and neutrophils to promote proinflammatory responses. *Blood*. 2005;105:1523–1530.
39. Oh H, Takagi H, Suzuma K, Otani A. Hypoxia and vascular endothelial growth factor selectively up-regulate angiopoietin-2 in bovine microvascular endothelial cells. *J Biol Chem*. 1999;274:15732–15739.
40. Willam C, Koehne P, Jurgensen JS, Grafe M. Tie2 receptor expression is stimulated by hypoxia and proinflammatory cytokines in human endothelial cells. *Circ Res*. 2000;87:370–377.
41. Enholm B, Paavonen K, Ristimaki A, Kumar V. Comparison of VEGF, VEGF-B, VEGF-C and Ang-1 mRNA regulation by serum, growth factors, oncoproteins and hypoxia. *Oncogene*. 1997;14:2475–2483.
42. Scott BB, Zaratin PF, Colombo A, Hansbury MJ. Constitutive expression of angiopoietin-1 and -2 and modulation of their expres-

sion by inflammatory cytokines in rheumatoid arthritis synovial fibroblasts. *J Rheumatol*. 2002;29:230–239.

43. Hangai M, He S, Hoffmann S, Lim JI. Sequential induction of angiogenic growth factors by TNF-alpha in choroidal endothelial cells. *J Neuroimmunol*. 2006;171:45–56.
44. Sarlos S, Rizkalla B, Moravski CJ, Cao Z. Retinal angiogenesis is mediated by an interaction between the angiotensin type 2 receptor, VEGF, and angiopoietin. *Am J Pathol*. 2003;163:879–887.
45. Hackett SF, Ozaki H, Strauss RW, Wahlin K. Angiopoietin 2 expression in the retina: upregulation during physiologic and pathologic neovascularization. *J Cell Physiol*. 2000;184:275–284.
46. Mandriota SJ, Pepper MS. Regulation of angiopoietin-2 mRNA levels in bovine microvascular endothelial cells by cytokines and hypoxia. *Circ Res*. 1998;83:852–859.
47. Otani A, Takagi H, Oh H, Koyama S. Angiotensin II induces expression of the Tie2 receptor ligand, angiopoietin-2, in bovine retinal endothelial cells. *Diabetes*. 2001;50:867–875.
48. Zhang L, Yang N, Park JW, Katsaros D. Tumor-derived vascular endothelial growth factor up-regulates angiopoietin-2 in host endothelium and destabilizes host vasculature, supporting angiogenesis in ovarian cancer. *Cancer Res*. 2003;63:3403–3412.
49. Pichiule P, Chavez JC, LaManna JC. Hypoxic regulation of angiopoietin-2 expression in endothelial cells. *J Biol Chem*. 2004;279:12171–12180.
50. Kim I, Kim JH, Ryu YS, Liu M. Tumor necrosis factor-[alpha] upregulates angiopoietin-2 in human umbilical vein endothelial cells. *Biochem Biophys Res Commun*. 2000;269:361–365.
51. Hackett SF, Wiegand S, Yancopoulos G, Campochiaro PA. Angiopoietin-2 plays an important role in retinal angiogenesis. *J Cell Physiol*. 2002;192:182–187.
52. Abdulmalek K, Ashur F, Ezer N, Ye F. Differential expression of Tie-2 receptors and angiopoietins in response to in vivo hypoxia in rats. *Am J Physiol*. 2001;281:L582–L590.
53. Romashkova JA, Makarov SS. NF-kappaB is a target of AKT in anti-apoptotic PDGF signalling. *Nature*. 1999;401:86–90.